



Storage of Electrical Information in Metal–Organic-Framework Memristors**

Seok Min Yoon, Scott C. Warren, and Bartosz A. Grzybowski*

Abstract: Single crystals of a cyclodextrin-based metal–organic framework (MOF) infused with an ionic electrolyte and flanked by silver electrodes act as memristors. They can be electrically switched between low and high conductivity states that persist even in the absence of an applied voltage. In this way, these small blocks of nanoporous sugar function as a non-volatile RRAM memory elements that can be repeatedly read, erased, and re-written. These properties derive from ionic current within the MOF and the deposition of nanometer-thin passivating layers at the anode flanking the MOF crystal. The observed phenomena are crucially dependent on the sub-nanometer widths of the channels in the MOF, allowing the passage of only smaller ions. Conversely, with the electrolyte present but no MOF, there are no memristance or memory effects.

Although metal–organic frameworks (MOFs) have emerged as an important platform for gas storage,^[1] catalysis,^[2] separations,^[3] and sensing,^[4] there are few examples of electrical devices, because most MOFs are insulators. By taking advantage of the periodic and porous structure of MOFs to trap and transport ions, we have identified a class of hybrid porous conductors with electrochemical properties that are unlike their purely solid or liquid counterparts. Herein, we show that a metal/MOF/metal heterostructure in which mobile ions are occluded into the MOF transforms it into an electrolyte with several unique properties. Most notably, the heterostructure can be electrically switched between low and high conductivity states persisting even in the absence of an applied voltage, and allowing for the switch to function as a non-volatile memory. Because these are two-terminal devices that exhibit hysteresis, except when no potential is applied (so-called pinched hysteresis), these devices are memristors, which are one of the four fundamental elements of electronic circuits.^[5,6] Our MOF memristors can be repeatedly read, erased, and re-written. Their ability to store information without any power input for several days

might be important in applications that require low power consumption.

Because most MOFs are insulators, to date they have been neglected as electronic materials for information processing. While several redox-active MOFs have been reported,^[7,8] their use as materials supporting electron transport is problematic because the changes in the redox state are usually accompanied by changes in the coordination number of a metal, which can lead to a non-reversible degradation of the MOF structure. Enabling ionic transport^[9,10] appears a more versatile approach, although this has been investigated to only a limited extent and has primarily relied on designing MOFs with built-in acid groups that impart proton conductivity. In the present work, ionic transport in a single-crystal MOFs infused with an ionic electrolyte is the key component of larger, metal/single-crystal MOF/metal heterostructures that act as non-volatile resistive random access memory (RRAM^[5,6,11,12]) elements. In a RRAM device, data is stored by inducing structural changes that switch the active material between a conductive “on” state and a non-conductive “off” state. As we demonstrate, the metal/single-crystal MOF/metal heterostructure also switches between high and low conductivity states owing to the self-limiting oxidative reactions of the metal anode.

We used γ -cyclodextrin based Rb-CD-MOF (Figure 1a) because of the ease with which millimeter-sized single crystals can be grown,^[13,14] enabling straightforward fabrication and testing of the MOF memory devices. Also, because Rb-CD-MOF is prepared in strongly basic conditions and contains free hydroxy ions in the as-synthesized material,^[13,14] we expected that infusing additional ions (for example, a metal hydroxide) into the pore network would enhance the ionic conductivity of the material without degrading the Rb-CD-MOF structure (Supporting Information, Figure S1). Accordingly, we infiltrated the MOF crystals with methanolic solutions of RbOH and deposited the RbOH by evaporating the solvent; Rb⁺ was chosen because it is already incorporated into the MOF structure whereby it coordinates to γ -CD (Supporting Information, Figure S2).^[13] To explore the electrical characteristics of the resulting devices, silver and/or gold electrical contacts were painted onto the opposite faces of the cubic MOF crystals using different colloidal pastes (Figure 1a,b).

The metal/MOF/metal heterostructures exhibited a range of electrical properties that are useful for the construction of a memory device. We begin by discussing the MOF loaded with a 100 mM solution of RbOH and electrically contacted using two silver electrodes (Figure 1a). Cyclic voltammetry scans^[7b] between -10 V and 10 V at ambient conditions (ca. 21°C , air with ca. 40% humidity; Figure 1c) showed that the

[*] Dr. S. M. Yoon, Dr. S. C. Warren, Prof. B. A. Grzybowski
Department of Chemistry and Department of Chemical and
Biological Engineering, Northwestern University
2145 Sheridan Rd., Evanston, IL 60208 (USA)
E-mail: grzybor@northwestern.edu
Homepage: <http://dysa.northwestern.edu>

[**] This work was supported by the Non-Equilibrium Energy Research
Center (NERC), which is an Energy Frontier Research Center funded
by the U.S. Department of Energy, Office of Science, Office of Basic
Energy Sciences under award DE-SC0000989.

Supporting information for this article is available on the WWW
under <http://dx.doi.org/10.1002/anie.201309642>.

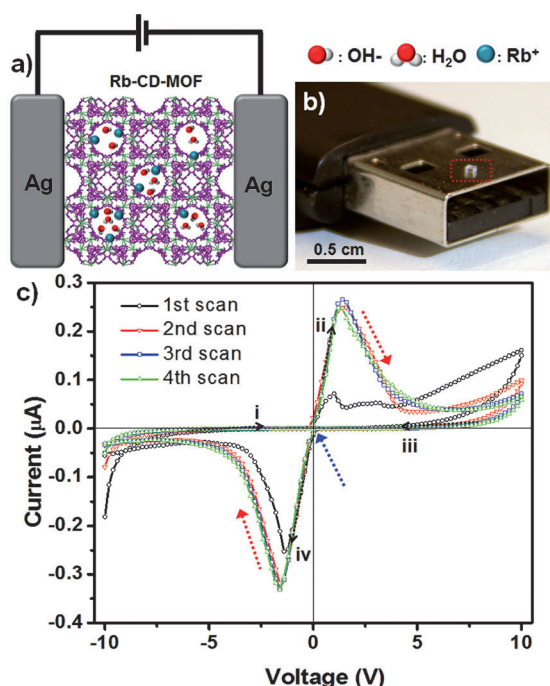


Figure 1. Construction of a memory device based on a metal–organic framework. a) A MOF memory device comprising two silver electrodes and Rb-CD-MOF crystal containing hydroxy ions, rubidium ions, and water. The device is not drawn to scale. b) A photograph of a circa 1 mm cubic Rb-CD-MOF crystal (in a red rectangle) placed on a flash memory stick. c) Cyclic voltammetry analysis of a silver/MOF/silver device heterostructure. The Rb-CD-MOF crystal was infiltrated with a 100 mM methanolic solution of RbOH and methanol was evaporated prior to electrical testing. A first cycle is needed to activate the device. Subsequent cycles exhibit negative differential resistance (red arrows) and pinched hysteresis^[26] with two hysteresis loops meeting at (0 V, 0 A) (indicated by the blue arrow).

first cycle is often poorly defined and exhibits only a modest degree of hysteresis. The device becomes fully activated and exhibits reproducible current–voltage behavior on subsequent cycles and maintains this for at least several hundred cycles. Scanning from 0 to 10 V, the current rises sharply up to about 2 V but then falls at higher voltages, which signifies an apparent decrease in conductivity and is a hallmark of so-called negative differential resistance, NDR.^[15–17] In the reverse voltage sweep, from 10 to 0 V, only a small current passes through the device and the resistance of the material is high. The scan continuing from 0→–10→0 V is symmetric with respect to the 0→10→0 V sweep. These observations indicate that there are two voltage windows in each cycle in which the device has a high apparent conductivity (0 to 2 V and 0 to –2 V) and two windows with a low apparent conductivity (2 to 10 to 0 V and –2 to –10 to 0 V). The switching between high and low conductivity gives rise to hysteresis but with an unusual feature in which the two hysteresis loops meet at an applied voltage of 0 V. Such a feature, which is referred to as “pinched” hysteresis, is characteristic of a memristor,^[5,6] which is an emerging class of two-terminal devices that are of interest for the design of electronic data storage devices. Memristors are an important

type of RRAM devices because the resistance of the material depends on the amount of current that has passed through the device, thereby providing a simple and potentially low-power way to switch the resistance of a material between two non-volatile states. While memristance has been observed in metal oxides (for example, TiO_x ,^[6,18] SiO_x ,^[11] ZnO ^[12]) and polymers,^[19] it has not been documented in porous materials, including MOFs.

To better understand the origin of this phenomenon in our MOF-based devices, we varied the concentration of RbOH that was deposited into the crystal pores. We found that memristance was most pronounced at high RbOH concentrations (Figure 2a) with the peak-to-valley current ratios 10, 4.5, and 2.5 for MOFs infiltrated using, respectively, 100 mM, 10 mM, and 0 mM RbOH in methanol (residual memristance for 0 mM can be attributed to the presence of hydroxy ions,^[14] eight for every γ -CD molecule,^[13] enabling ionic conductivity). Memristance was also most clearly observed when the experiments were performed in humidified nitrogen or air, but these features entirely disappeared in dry nitrogen and dry oxygen (green and red markers in Figure 2b). The dependence of memristance on the ion concentration and water content (Supporting Information, Figure S4), suggests that conduction through the MOF requires ion movement; in the absence of water, the dissociation energy of RbOH into Rb^+ and OH^- is large, and the material is highly resistive.

The requirement of ion movement identifies the principle of the conduction mechanism through the MOF but does not explain why the resistance changes. To answer this question, we fabricated devices in which the two electrodes were made of gold. In this case, the current increased monotonically with voltage, the magnitudes of the currents were considerably lower, and memristance was not observed (Figure 2c, curve iii). This suggested that the change in material structure that underlies memristance occurs only at the silver/MOF interface but not at the gold/MOF interface. To explore this hypothesis further, devices were built using one gold electrode and one silver electrode (Figure 2c, curves i and ii). In this case, a single large hysteresis loop was observed only when a positive voltage was applied to the silver electrode. When the gold and silver electrodes were exchanged, the large hysteresis loop was observed under the opposite polarization conditions (Figure 2c, curves i and ii). These observations indicate that the change in the apparent resistance of the device is due to an oxidation process that occurs at the interfaces between the MOF and the silver anode.

Under basic conditions and at positive potentials, silver grows a layer of silver hydroxide (AgOH) and silver oxide (AgO_x) on its surface (Figure 2d; Supporting Information, Figure S3).^[20,21] By carefully delaminating the MOF from both the anode and the cathode and performing XPS on each (Supporting Information, Figure S3), we confirmed that silver oxidation occurs only at the silver anode/MOF interface. The process is self-limiting because further oxidation requires mass transport of hydroxide ions through the oxidized layer. The Faradaic current from the oxidation of silver is much larger than the capacitive movement of ions near the metal electrode (which is the primary source of current near the gold electrodes, as evidenced by the fact that after the silver

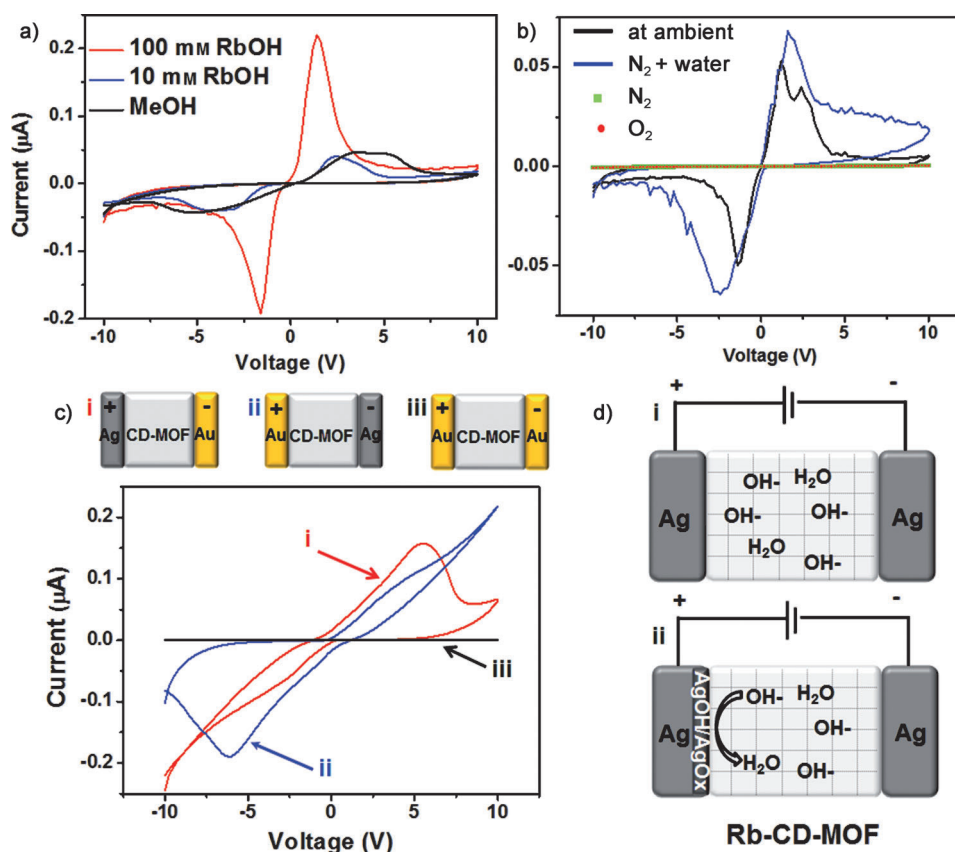


Figure 2. Operating mechanism of the MOF-based memory. a) Well-defined switching behavior and negative differential resistance require addition of ca. 100 mM RbOH. All of the devices were tested under ambient conditions with a scan rate of 0.07 V s^{-1} and silver electrodes. b) Electrical properties under different gas atmospheres used. In each case, a silver/MOF/silver device was immersed in a 100 mM RbOH methanol solution and the solvent was evaporated; all scan rates were 0.07 V s^{-1} . Electrical characteristics are compared for ambient conditions (black line), humidified nitrogen (blue), dry oxygen (red), and dry nitrogen (green). c) Cyclic voltammetry was performed on metal/MOF/metal structures in which the electrodes were made of (i) silver/gold, (ii) gold/silver, and (iii) gold/gold. Experiments were performed under ambient conditions with a scan rate of 0.07 V s^{-1} and with 100 mM RbOH loaded into the MOF. The experiments reveal that memristor-type hysteresis and NDR require a positive (anodic) potential to be applied to silver, leading to its oxidation. d) A model of the electrochemical mechanism that leads to the switching behavior and memory effect in Ag/MOF/Ag devices. (i) Upon applying a small voltage, charge transport occurs and is primarily driven by the movement of ions. (ii) Large positive voltages lead to the oxidation of the silver, producing a resistive silver hydroxide/oxide insulating layer that impedes further charge transport until a negative voltage is applied that reduces silver hydroxide/oxide back to silver.

electrode has been fully oxidized, the small current through the silver/MOF/silver device is nearly identical to that through the gold/MOF/gold device). As a result of Ag oxidation and its gradual passivation, the initial current rise with increasing voltage is followed by a current decrease. Then, as long as the same polarization of the voltage is maintained, the current remains small and the device has a high apparent resistance. When the polarization is inverted, however, the silver oxide layer is reduced and the other electrode is gradually oxidized. This results in a large current flow that then decays as these Faradaic processes come to completion (Figure 3a–e). This model is consistent with the magnitude of the currents that are passed during an oxidation/reduction process: during a voltage excursion from 0 to 10

0 V, the quantity of the charge that is passed corresponds to the oxidation of about 10 to 30 nanometers of silver, depending on the scan rate.

Importantly, control experiments (Supporting Information, Figure S5) show that memristor behavior is only observed at a MOF crystal/Ag electrode interface and not at an interface between Ag and an liquid electrolyte solution. Similarly, no memristance is observed when polycrystalline MOF pellets are used instead of a single crystal. These observations and the thermodynamic instability of the $\text{Ag}(\text{OH})/\text{AgO}_x$ layer under the conditions we use^[22] all indicate that memristance depends on selective ion transport through the sub-nanometer channels of the MOF. In this scenario, the channels permit the passage of small hydroxide ions but limit that of hydrated Ag^+ (of a size commensurate with the channel diameter^[23]) dissolving from the hydrated $\text{Ag}(\text{OH})/\text{AgO}_x$ layer. Therefore, the MOF/Ag interface promotes the passivation of the anode by the $\text{Ag}(\text{OH})/\text{AgO}_x$ layer more than the electrolyte solution/Ag interface, from which the Ag^+ ions can migrate freely.

With this mechanistic understanding, we demonstrated the ability to write, read, and erase data in the Ag/MOF/Ag memristor. To write an “on” or “1” state, the voltage was scanned from 0 V to –10 V.

This led to the oxidation of the “right” electrode and reduction of the left electrode in Figure 3b. When a positive voltage of 2 V to 4 V was then applied (vertical dashed lines in Figure 3a), a large Faradaic current passed as the left electrode began to oxidize (Figure 3c); this large current corresponded to the reading of the “1” state. Alternatively, to write an “off” or “0” state, the device was scanned from 0 V → 10 V. This yielded the state in which the right electrode was reduced and the left oxidized (Figure 3d). When this state was read by applying a positive voltage, no Faradaic current passed because the anode had already been oxidized (Figure 3e).

Three different scan rates were studied, but, regardless of the scan rate, similar amounts of charge were passed,

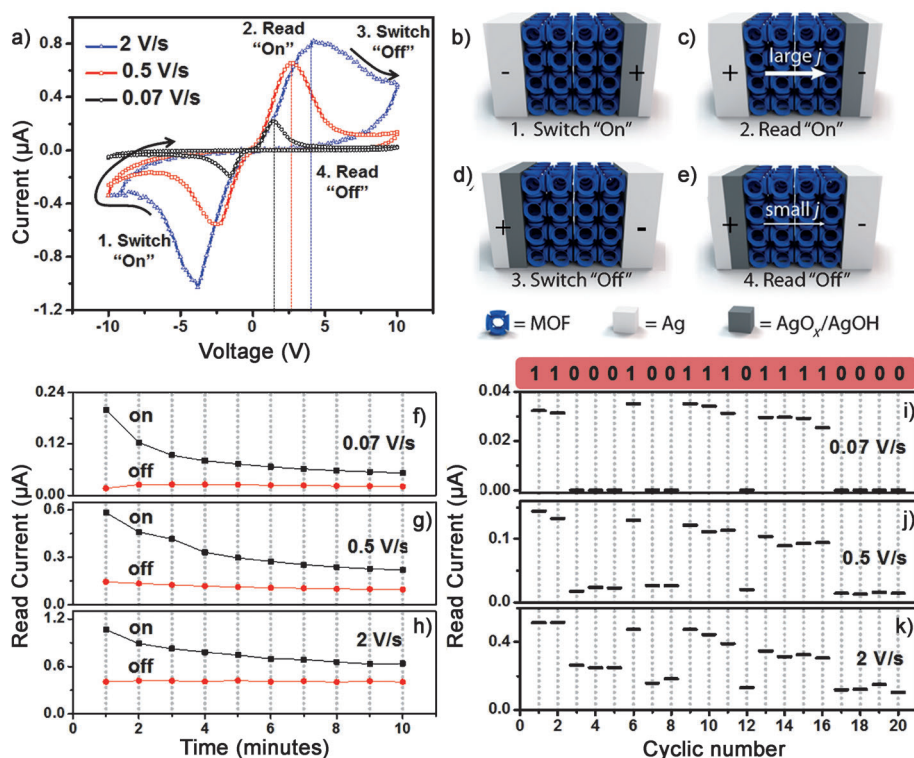


Figure 3. An electrically addressable MOF memory illustrating reading, writing, and erasing capabilities as well as random access memory with a random read/write sequence. a) Cyclic voltammetry is shown for three different scan speeds of a Rb-CD-MOF device flanked by silver electrodes infused with 100 mM RbOH. b)–e) In a full cycle (for example, $0\text{ V} \rightarrow 10\text{ V} \rightarrow -10\text{ V} \rightarrow 0\text{ V}$), the system passes through two highly conductive states and two non-conductive states. For application as a memory device, we only use one set of these states, which are read at positive voltages. b) The device is switched to a conductive “on” state by sweeping to -10 V and returning to a small positive voltage. d) The device is switched to a non-conductive “off” state by sweeping the voltage to 10 V . The (c) “on” and (e) “off” states are read at the voltage marked by the vertical lines in (a). f)–h) A “0” or “1” (i.e., off or on) state was written into the MOF memory and repeatedly read. The data was written and read at a scan rate of 0.07 V s^{-1} (f), 0.5 V s^{-1} (g), and 2 V s^{-1} (h); these experiments were performed in air. i)–k) Data bits were written into the silver/MOF/silver device according to an arbitrarily chosen sequence: “11000100111011110000”. After each write sequence, the data was read by recording the current (read current, y-axis) as described in (a). After reading a “1”, voltage was swept from $0\text{ V} \rightarrow -10\text{ V}$ at 0.07 V s^{-1} (i), 0.5 V s^{-1} (j), and 2 V s^{-1} (k) to re-reduce the silver oxide that had formed at the anode. The on/off ratio is the ratio of currents between a “1” and a “0”. i) This value approached 150 for a read/write speed of 0.07 V s^{-1} . The ratio decreased to 10 (j) and 2 (k) for faster read/write speeds because of the increased contribution to current from capacitance.

reflecting the production of passivating layers of roughly similar thickness by a pseudocapacitive current. To examine whether the data was non-volatile, after writing either a “0” or “1” at time = 0, the data was repeatedly read at 1 min intervals (Figure 3 f–h). A written “0” did not change, regardless of the number of times it was read. In contrast, a written “1” decayed with time because the process of reading this value gradually oxidizes the reduced electrode and reduces the oxidized electrode, thereby converting the “1” into a “0”. Reading the data at higher scan rates (that is, with less current passing and less oxidation occurring) alleviated the problem only marginally (Figure 3 f–h). On the other hand, the lifetime of 1 s could be improved significantly by sweeping the voltage to -10 V after each read event and thus refreshing the “1” state. Automating this

procedure allowed writing and reading binary sequences such as those shown in Figure 3 i–k. The best quality of data storage (lasting up to a week) was achieved when this refreshing procedure was combined with the encapsulation of the MOF in an epoxy resin (Figure 4; Supporting Information, Figure S6b). This procedure preserved the original water content in the MOF and prevented any additional water from entering, which would lead to the dissolution of the silver oxide phase.

In summary, we have constructed the first example of an electrically addressable MOF-based memory with modest volatility. Addition of mobile ions to a MOF transforms this hybrid material into a unique electrolyte in which the nanoscopic channels of the MOF limit the migration of larger ions (here, hydrated Ag^+) while still supporting the flow of both capacitive and faradaic currents. The major limitation of our proof-of-the-concept system is that the read/write times are slow (seconds) compared to state-of-the-art memristors (ns to μs). We suggest, however, that these times can be improved by improving the kinetics for oxidation/reduction as well as reducing the total amount of material needed to block current transport. Towards this end, smaller MOF crystals and the use of metals with faster kinetics for self-passivation seem most promising. These MOF based memory devices have exceptional prospects for miniaturization in all dimensions

because the writing of bits is achieved at a few nanometers of the MOF/metal interface. Furthermore, high density data storage in MOF memristors could be realized by patterning multiple electrodes on the MOFs by techniques such as wet stamping.^[24,25]

Received: November 5, 2013

Published online: March 13, 2014

Keywords: memristors · metal–organic frameworks · negative differential resistance · non-volatile memory · resistive random access memory

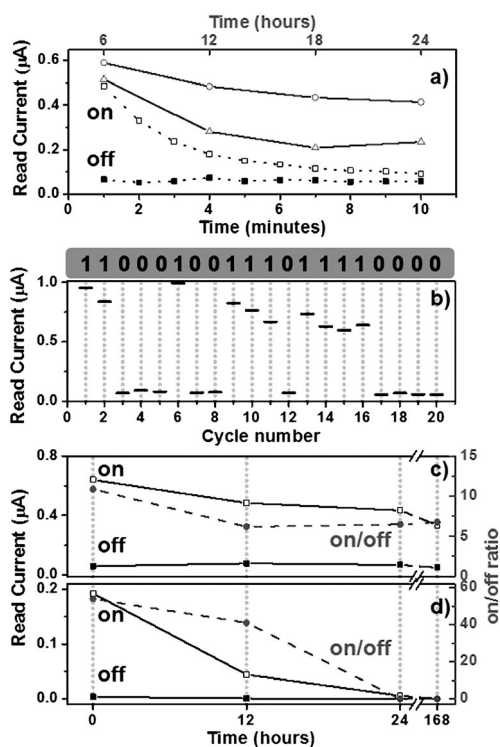


Figure 4. Durability of encapsulated MOF memory device and non-volatile memory storage. a) “0” or “1” (off or on) states were written into epoxy-encapsulated MOF crystals and read every 6 h for 24 h total (solid lines). The lower middle “on” curve is for a situation where the “1 s” are not refreshed by applying a negative voltage after every reading; in the top “on” curve, the “1 s” are refreshed after every reading. Although in both cases the “1 s” decay much slower than for non-encapsulated MOFs (dotted lines, compare Figure 3 f–h), the performance of our MOF memory elements is optimal with encapsulation and with refreshing. The data was written and read at 3 V with a scan rate of 0.07 V s^{-1} . b) RAM performance of the epoxy-encapsulated MOF memory device for a randomly selected sequence of 1 s and 0 s. The MOF RAM device showed an average on/off ratio of 10. The data was written and read at 3 V with a scan rate of 0.07 V s^{-1} . c) and d) Persistence of the “1” and “0” states (solid lines) and on/off ratio (dashed lines) of (c) the epoxy-encapsulated MOF RAM device and (d) the bare MOF RAM device. While non-encapsulated devices typically failed within 24 h, the memory persisted for over 1 week (168 h) when the MOF was encapsulated, demonstrating non-volatile memory storage.

- [1] a) H. Li, M. Eddaoudi, M. O’Keeffe, O. M. Yaghi, *Nature* **1999**, *402*, 276–279; b) N. L. Rosi, J. Eckert, M. Eddaoudi, D. T. Vodak, J. Kim, M. O’Keeffe, O. M. Yaghi, *Science* **2003**, *300*, 1127–1129; c) M. P. Suh, H. J. Park, T. K. Prasad, D. W. Lim, *Chem. Rev.* **2011**, *111*, 782–835; d) K. Sumida, D. L. Rogow, J. A. Mason, T. M. McDonald, E. D. Bloch, Z. R. Herm, T. H. Bae, J. R. Long, *Chem. Rev.* **2011**, *111*, 724–781.
- [2] a) J. S. Seo, D. Whang, H. Lee, S. I. Jun, J. Oh, Y. J. Jeon, K. Kim, *Nature* **2000**, *404*, 982–986; b) S. Horike, M. Dincă, K. Tamaki, J. R. Long, *J. Am. Chem. Soc.* **2008**, *130*, 5854–5855.

- [3] a) J. R. Li, J. Sculley, H. C. Zhou, *Chem. Rev.* **2011**, *111*, 869–932; b) S. Han, Y. Wei, C. Valente, I. Lagzi, J. J. Gassensmith, A. Coskun, J. F. Stoddart, B. A. Grzybowski, *J. Am. Chem. Soc.* **2010**, *132*, 16358–16361.
- [4] L. E. Kreno, K. Leong, O. K. Farha, M. Allendorf, R. P. Van Duyne, J. T. Hupp, *Chem. Rev.* **2011**, *111*, 1105–1125.
- [5] a) L. Chua, *IEEE Trans. Circuit Theory* **1971**, *18*, 507–509; b) T. Prodromakis, C. Toumazou, L. Chua, *Nat. Mater.* **2012**, *11*, 478–481.
- [6] D. B. Strukov, G. S. Snider, D. R. Stewart, R. S. Williams, *Nature* **2008**, *453*, 80–83.
- [7] a) H. R. Moon, J. H. Kim, M. P. Suh, *Angew. Chem.* **2005**, *117*, 1287–1291; *Angew. Chem. Int. Ed.* **2005**, *44*, 1261–1265; b) A. Dragässer, O. Shekhah, O. Zybalyo, C. Shen, M. Buck, C. Woll, D. Schlottwein, *Chem. Commun.* **2012**, *48*, 663–665.
- [8] M. Tonigold, Y. Lu, B. Bredenkötter, B. Rieger, S. Bahn Müller, J. Hitzbleck, G. Langstein, D. Volkmer, *Angew. Chem.* **2009**, *121*, 7682–7687; *Angew. Chem. Int. Ed.* **2009**, *48*, 7546–7550.
- [9] S. Bureekaew, S. Horike, M. Higuchi, M. Mizuno, T. Kawamura, D. Tanaka, N. Yanai, S. Kitagawa, *Nat. Mater.* **2009**, *8*, 831–836.
- [10] J. A. Hurd, R. Vaidhyanathan, V. Thangadurai, C. I. Ratcliffe, I. L. Moudrakovski, G. K. H. Shimizu, *Nat. Chem.* **2009**, *1*, 705–710.
- [11] W. I. Park, J. M. Yoon, M. Park, J. Lee, S. K. Kim, J. W. Jeong, K. Kim, H. Y. Jeong, S. Jeon, K. S. No, J. Y. Lee, Y. S. Jung, *Nano Lett.* **2012**, *12*, 1235–1240.
- [12] J. Song, Z. Yan, C. Xu, W. Wu, Z. L. Wang, *Nano Lett.* **2011**, *11*, 2829–2834.
- [13] R. A. Smaldone, R. S. Forgan, H. Furukawa, J. J. Gassensmith, A. M. Z. Slawin, O. M. Yaghi, J. F. Stoddart, *Angew. Chem.* **2010**, *122*, 8812–8816; *Angew. Chem. Int. Ed.* **2010**, *49*, 8630–8634.
- [14] Y. H. Wei, S. B. Han, D. A. Walker, P. E. Fuller, B. A. Grzybowski, *Angew. Chem.* **2012**, *124*, 7553–7557; *Angew. Chem. Int. Ed.* **2012**, *51*, 7435–7439.
- [15] J. Chen, M. A. Reed, A. M. Rawlett, J. M. Tour, *Science* **1999**, *286*, 1550–1552.
- [16] Q. Tang, H. K. Moon, Y. Lee, S. M. Yoon, H. J. Song, H. Lim, H. C. Choi, *J. Am. Chem. Soc.* **2007**, *129*, 11018–11019.
- [17] J. He, S. M. Lindsay, *J. Am. Chem. Soc.* **2005**, *127*, 11932–11933.
- [18] J. J. Yang, M. D. Pickett, X. Li, D. A. A. Ohlberg, D. R. Stewart, R. S. Williams, *Nat. Nanotechnol.* **2008**, *3*, 429–433.
- [19] T. Berzina, A. Smerieri, M. Bernabò, A. Pucci, G. Ruggeri, V. Erokhin, M. P. Fontana, *J. Appl. Phys.* **2009**, *105*, 124515.
- [20] R. Memming, F. Mollers, G. Neumann, *J. Electrochem. Soc.* **1970**, *117*, 451–457.
- [21] X. Y. Gao, S. Y. Wang, J. Li, Y. X. Zheng, R. J. Zhang, P. Zhou, Y. M. Yang, L. Y. Chen, *Thin Solid Films* **2004**, *455–456*, 438–442.
- [22] M. Pourbaix, *Atlas of electrochemical equilibria in aqueous solutions*, Cebalcor, **1974**.
- [23] I. Persson, *Pure Appl. Chem.* **2010**, *82*, 1901–1917.
- [24] S. Han, Y. Wei, C. Valente, R. S. Forgan, J. J. Gassensmith, R. A. Smaldone, H. Nakanishi, A. Coskun, J. F. Stoddart, B. A. Grzybowski, *Angew. Chem.* **2011**, *123*, 290–293; *Angew. Chem. Int. Ed.* **2011**, *50*, 276–279.
- [25] C. J. Campbell, S. K. Smoukov, K. J. M. Bishop, E. Baker, B. A. Grzybowski, *Adv. Mater.* **2006**, *18*, 2004–2008.
- [26] Pinched hysteresis is characteristic of a memristor. Of the twenty devices tested, 90 % exhibited this behavior; the remaining 10 % exhibited either no current or other non-memristive behavior, which is likely to be due to the presence of structural defects (for example, cracks) within the MOF that limit charge transport.